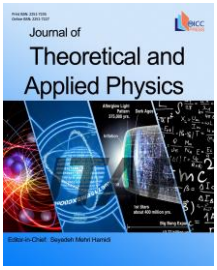

J. Theor. Appl. Phys., 2026; 20(2): 196-205

Journal of Theoretical and Applied Physics (JTAP)

https://doi.org/10.57647/jtap.2026.2002.17

Research Article

Propagation Characteristics of Higher-Order Hollow Sinh-Gaussian Laser Beams in Collisionless Plasma

Prajakta P. Patil[1], Mansing V. Takale[2], Sandip D. Patil[1,*]

[1]*Department of Physics, Devchand College, Arjunnagar 591 237, Maharashtra, India*
[2]*Department of Physics, Shivaji University, Kolhapur 416 004, Maharashtra, India*

***Corresponding author:** sdpatil_phy@rediffmail.com

Article History:

Received:
24 October 2025

Revised:
21 December 2025

Accepted:
25 December 2025

Published Online:
05 February 2026

Published in Issue:
30 April 2026

Abstract

Hollow sinh-Gaussian (HshG) beams are the appropriate analogue to describe optical beams with null central intensity. In the present work, the modified paraxial approach is adopted to study the propagation characteristics of higher-order HshG beams in plasma. The nonlinearity in the dielectric constant of plasma considered herein is of the ponderomotive type. A nonlinear differential equation is obtained for the beam-width parameter and then solved numerically to investigate the self-focusing/defocusing characteristics of HshG beams in plasma. The dependence of the beam-width parameter of HshG beams on the dimensionless distance of propagation through plasma has been specifically carried out. Results show that the self-focusing ability of the aforesaid beams weakens with an increase in the order of HshG beams. The effect of the initial intensity parameter and the normalized plasma frequency for higher-order HshG beams has also been examined.

Keywords: Hollow sinh-Gaussian beams, Self-focusing, Ponderomotive nonlinearity, Collisionless plasma, Modified paraxial

Cite this article: Patil, P. P.,Takale, M. V. & Patil, S. D., (2026). Propagation characteristics of higher-order hollow sinh-Gaussian laser beams in collisionless plasma. *J. Theor. Appl. Phys.,* 20(2), 196-205. https://doi.org/10.57647/jtap.2026.2002.17

1. Introduction

In the past two decades, there has been a significant surge in wide-ranging research interest exploring the potential of high-intensity laser beams and specifically their interactions with plasmas. Many distinctive characteristics of laser beams give rise to various nonlinear phenomena, profoundly influencing laser-plasma interactions, offering diverse applications such as high-order harmonic generation [1], laser-driven inertial confinement fusion [2], laser wakefield acceleration [3], terahertz radiation generation [4], etc. Consequently, the growing applications of laser technologies require the development of high-intensity laser systems that employ the chirped-pulse amplification technique [5]. Self-focusing [6, 7] is one of the important nonlinear optical phenomena in the laser-plasma interaction processes, because the nonlinear effects are highly sensitive to the irradiance distribution along the wavefront of the beam. Before proceeding further, it is instructive to highlight the ponderomotive nonlinearity responsible for self-focusing in plasma. In a collisionless plasma, a redistribution of electron density results from the ponderomotive force acting on electrons, which is proportional to the gradient of irradiance along the

wavefront of the beam. This, in turn, causes the modification in the dielectric constant of plasma [8]. This nonlinearity sets in the period on the order of r_0/c_s, where r_0 is the width of the beam and c_s is the ion sound speed. Other nonlinear mechanisms are also significant in various physical situations of laser-plasma interaction, thereby causing modifications in the dielectric constant of the plasma. The beam spreads substantially in several Rayleigh diffraction lengths R_d $(\sim kr_0^2)$ in the absence of nonlinearities, where k is the wave number. This tendency of the beam to spread due to diffraction balances the self-focusing. So far, the primary focus of both theoretical and experimental investigations on the self-focusing laser beam in plasma has been directed towards the propagation characteristics of the Gaussian-shaped laser beam. All nonlinear phenomena related to laser-plasma interaction depend on the input form of the laser beam intensity profile. As a result, lasers with a certain intensity profile and appropriate characteristic features are essential. The intensity profile of the laser beam accounts for several possible deviations from the Gaussian distribution for specific applications. There have been prior attempts to ascertain the propagation properties of various modified Gaussian beams.

Additionally, Cai et al.[9, 10] proposed a hollow Gaussian beam and showed their unique properties, featured applications, and method of generation. On the theoretical side, Sodha et al.[11] developed a modified paraxial approach for the phenomenon of self-focusing of hollow Gaussian (DHG) beams by expanding relevant parameters in the vicinity of the intensity maximum. On the other side, experimental observations by Tan et al.[12] confirmed the ring-like structure of the laser beam. It is well-known that the paraxial approach for self-focusing of a laser cannot account for the changing radial profile of the laser beam from an initial Gaussian to that of ring shaped. This enables subsequent use of the modified paraxial approach for self-focusing in a number of investigations. Sharma et al.[13] presented the evaluation of thermal defocusing of DHG beams in the atmosphere. Hong et al.[14] studied the propagation characteristics of DHG laser beams in a tapered plasma channel. They found that the focusing ability of the hollow Gaussian beams is proportional to the density of the tapered plasma channel. The present status of self-focusing of DHG beams comprises significant interest in harmonic generation [15], electron plasma wave excitation [16], ion acceleration [17], and generation of terahertz radiation [18]. Another representation of the novel candidate beams is the hollow sinh-Gaussian (HshG) beams. These are usually hollow Gaussian beams that exhibit a transverse intensity distribution characterized by a single ring structure.

The intensity profile of the HshG beams also shows a bright annular ring with zero central intensity. Subsequently, HshG beams have been extensively investigated in various theoretical and experimental studies.

Sun et al.[19] examined HshG beams and their paraxial properties. Their result showed that a single bright ring well defines the intensity profile of HshG beams, and its size depends on the order of the beam.

The shape of the ring can also be controlled, leading to the elliptical HshG beams. Tang et al.[20] investigated propagation characteristics of the HshG beams through a fractional Fourier transform (FRFT) optical system. They reported that the normalized intensity distribution of the HshG beams in the FRFT plane is closely related to the order of the beam. Zou et al.[21] studied the propagation properties of HshG beams in a quadratic-index medium. They observed that HshG beams can also maintain their initial dark hollow structure for higher orders.

Zhu et al.[22] showed that the perfect hollow configuration of dark hollow structures of HshG beams can retain a quite long propagating distance under small complex beam parameters. In previous studies [9-14], the interaction of HshG beams with plasma has not been adequately reflected.

These studies are based on Gaussian, dark-hollow, or Hermite–cosh Gaussian beams with different radial intensity patterns. The intensity profile of HshG beams exhibit a rapidly increasing hyperbolic-sine function along with usual Gaussian function. Sun et al.[19] and Zou et al.[21] examined HshG beams only in linear optical media, neglecting plasma effects. Here, we investigate the propagation of HshG beams in nonlinear plasma, explicitly accounting for beam–medium interaction. Therefore, in this work, a self-consistent theoretical model for the evaluation of the beam-width parameter of HshG beams in collisionless plasma has been presented.

The dependence of the initial intensity parameter and normalized plasma frequency on self-focusing of HshG beams has been considered. The paper is organized as follows: In Sec. 2, the electric field distribution of the HshG beams, the nonlinear dielectric function of collisionless plasma, and the evaluation of beam spot size have been studied under a modified paraxial approach for the phenomenon of self-focusing. In Sec. 3, the numerical results for self-focusing and defocusing of HshG beams are discussed. Finally, conclusions are presented in Sec. 4.

2. Analytical investigation

The initial electric field distribution of the HshG beams in a cylindrical coordinate system can be written as [19]:

$$E(r,0) = E_0 sinh^n\left(\frac{r}{r_0}\right) exp\left(-\frac{r^2}{2r_0^2}\right) exp(i\omega t) \quad (1)$$

where r is the radial coordinate, r_0 is the initial beam radius, $sinh^n(\cdot)$ represents the hyperbolic sine function, n is the beam's order characterizing the shape of HshG beams and the position of the maximum, ω is the wave frequency, E_0 is a constant amplitude of the HshG beams, which describes the electric field maximum at $r = r_{max} = r_0 n$. This generalization appears reasonably good approximation that demands the inequality $n \geq 1$ for higher-order HshG beams in the present investigation.

Following Sodha et al.[11], The effective dielectric function describing ponderomotive nonlinearity in a collisionless plasma can be expressed as:

$$\varepsilon(\eta, z) = 1 - \Omega^2 exp(-\beta E E^*) \quad (2)$$

where $\Omega = \omega_p/\omega$, $\omega_p = (4\pi n_0 e^2/m)^{1/2}$ is the electron plasma frequency, e and m are charge and rest mass of the electron, respectively. n_0 is the undisturbed density of plasma electrons, and $\beta = (3/4)\, m\alpha/M$ is the coefficient of pondermotive nonlinearity with $\alpha = e^2/8m\omega^2 k_B T_o$. Here, M is the mass of the ion, k_B is the Boltzmann constant and T_o is the plasma temperature.

The propagation of a laser beam in plasma is described by the following wave equation:

$$\nabla^2 E + \frac{\omega^2}{c^2}\varepsilon(r,z)E = 0 \quad (3)$$

Within the framework of the WKB approximation, the solution of Eq. (3) can be expressed as $E(r,z) = A(r,z)exp(-i\int k(z)dz)$, where $A(r,z)$ is the complex amplitude of the electric field and $k(z)$ is the wave vector. Substituting $E(r,z)$ in Eq. (3) and neglecting the term $(\partial^2 A/\partial z^2)$ by assuming $A(r,z)$ to be a slowly varying function of z, one obtains:

$$2ik\frac{\partial A}{\partial z} + iA\frac{\partial S}{\partial z} = \nabla_\perp^2 A + \frac{\omega^2}{c^2}(\varepsilon - \varepsilon_0) \quad (4)$$

The complex amplitude $A(r,z)$ may be expressed as $A(r,z) = A_0(r,z)exp[-ik(z)S(r,z)]$, where $S(r,z)$ is termed the eikonal associated with HshG beams. The modified paraxial approximation is governed by the small-angle condition $|\nabla_\perp^2 A| \ll kA$ and the slowly varying envelope requirement, i.e. $|\partial A/\partial z| \ll kA$.

These conditions depend on the characteristic transverse scale r_0 relative to the wavelength λ and not explicitly on the beam order n.

Although an increase in n shifts the intensity maximum of HshG beams away from the axis, the characteristic transverse variation in the vicinity of the annular peak remains on the order $1/r_0$, ensuring modified paraxial propagation for $r_0 \gg \lambda$.

Substituting $A(r,z)$ in Eq. (4) and the separation of the real and imaginary parts, yields:

$$\frac{2S}{k}\frac{\partial k}{\partial z} + 2\frac{\partial S}{\partial z} + \left(\frac{\partial S}{\partial r}\right)^2 = \frac{1}{k^2 A_0}\left(\frac{\partial^2 A_0}{\partial r^2} + \frac{1}{r}\frac{\partial A_0}{\partial r}\right) + \frac{\omega^2}{k^2 c^2}(\varepsilon - \varepsilon_0) \quad (5a)$$

and

$$\frac{\partial A_0^2}{\partial z} + A_0^2\left(\frac{\partial^2 S}{\partial r^2} + \frac{1}{r}\frac{\partial S}{\partial r}\right) + \frac{\partial A_0^2}{\partial r}\frac{\partial S}{\partial r} + \frac{A_0^2}{k}\frac{\partial k}{\partial z} = 0 \quad (5b)$$

To describe the beam dynamics locally around the annular intensity maximum, we adopt a modified paraxial approach developed by Sodha et al.[11] for focusing of DHG beams in plasma. Thus, one can transform (r,z) coordinates into (η,z) coordinates by the relation,

$$\eta = [(r\ /\ r_0\, f) - n] \quad (6)$$

where $f(z)$is the beam-width parameter of HshG beams. The coordinate $\eta = 0$ corresponds to the instantaneous position of maximum irradiance, and the present analysis is restricted to the near-peak region $\eta \ll n$.

Thus, from Eqs (5a), (5b) and (6) one obtains,

$$\frac{2S}{k}\frac{\partial k}{\partial z} + 2\frac{\partial S}{\partial z} + \frac{1}{r_0^2 f^2}\left(\frac{\partial S}{\partial \eta}\right)^2 = \frac{1}{k^2 A_0 r_0^2 f^2}\left(\frac{\partial^2 A_0}{\partial \eta^2} + \frac{1}{(n+\eta)}\frac{\partial A_0}{\partial \eta}\right) + \frac{\omega^2}{k^2 c^2}(\varepsilon - \varepsilon_0) \quad (7a)$$

and

$$\frac{\partial A_0^2}{\partial z} + \frac{A_0^2}{r_0^2 f^2}\left(\frac{\partial^2 S}{\partial \eta^2} + \frac{1}{(n+\eta)}\frac{\partial S}{\partial \eta}\right) + \frac{\partial A_0^2}{\partial \eta}\frac{\partial S}{\partial \eta} + \frac{A_0^2}{k}\frac{\partial k}{\partial z} = 0 \quad (7b)$$

In the paraxial-like approximation, the relevant parameters may be expanded around the position of the maximum of the irradiance of HshG beams, i.e., around $\eta = 0$. Thus, the dielectric function $\varepsilon(\eta,z)$ can be expressed around $\eta = 0$ as

$$\varepsilon(\eta, z) = \varepsilon_0(z) - \eta^2 \varepsilon_2(z) \quad (8)$$

where ε_0 and ε_2 are the coefficients associated with η^0 and η^2 in the expansion of $\varepsilon(\eta,z)$, respectively.

Thus, one can write from Eqs. (2) and (8) as

$$\varepsilon_0 = \varepsilon(\eta = 0, z) \quad (9a)$$

and

$$\varepsilon_2 = \left(\frac{\partial \varepsilon(\eta,z)}{\partial \eta^2}\right)_{\eta=0} \quad (9b)$$

To obtain a specific expression for the above coefficient, one may expand EE^* in powers of η^2; thus:

$$EE^* = A_0^2 \approx g_0(z) - \eta^2 g_2(z) \tag{10}$$

Here, coefficients $g_0(z)$ and $g_2(z)$ may expressed as

$$g_0(z) = \frac{E_0^2}{f^2}\, e^{-n^2} sinh(n)^{2n} \tag{11}$$

and

$$g_2(z) = \frac{E_0^2}{2f^2}\, e^{-n^2} sinh(n)^{-2+2n} C \tag{12}$$

Where $C = [1 - 2n + (-1 + 4n^2)cosh(2n) - 4n^2 sinh(2n)]$ With the help of Eq.(11) and (12), one can easily obtain $\varepsilon_0(z)$ and $\varepsilon_2(z)$ for pondermotive nonlinearity as

$$\varepsilon_0(z) = 1 - \Omega^2 e^{(-\alpha\beta g_0)} \tag{13a}$$

and

$$\varepsilon_2(z) = 2\Omega^2\, e^{-2n(1+n)} e^{(-\alpha\beta g_0)} (\alpha^2\beta^2 g_0^2 - \alpha\beta g_2) \tag{13b}$$

Substituting $\varepsilon(\eta, z)$ from Eq. (8) in Eqs. (7a) and (7b) lead to:

$$\frac{2S}{k}\frac{\partial k}{\partial z} + 2\frac{\partial S}{\partial z} + \frac{1}{r_0^2 f^2}\left(\frac{\partial S}{\partial \eta}\right)^2 = \frac{1}{k^2 A_0 r_0^2 f^2}\left(\frac{\partial^2 A_0}{\partial \eta^2} + \frac{1}{(n+\eta)}\frac{\partial A_0}{\partial \eta}\right) - \eta^2 \frac{\omega^2}{k^2 c^2}(\varepsilon_2) \tag{14a}$$

and

$$\frac{\partial A_0^2}{\partial z} + \frac{A_0^2}{r_0^2 f^2}\left(\frac{\partial^2 S}{\partial \eta^2} + \frac{1}{(n+\eta)}\frac{\partial S}{\partial \eta}\right) + \frac{1}{r_0^2 f^2}\frac{\partial A_0^2}{\partial \eta}\frac{\partial S}{\partial \eta} + \frac{A_0^2}{k}\frac{\partial k}{\partial z} = 0 \tag{14b}$$

It is interesting to note that the maximum irradiance of HshG beams is located at $\eta = 0$ that corresponds to the position of the maximum irradiance for the propagating beams via $r = r_0 fn$. We consider the following ansatz in terms of the new variables (η, z) as:

$$A_0^2(\eta, z) = \frac{E_0^2}{f^2} sinh(n+\eta)^{2n} exp\left(-\frac{(n+\eta)^2}{2}\right) \tag{15}$$

$$S(\eta, z) = \frac{(n+\eta)^2}{2} r_0^2 f \frac{df}{dz} + \varphi(z) \tag{16}$$

where $\varphi(z)$ is an arbitrary function of z.
On substituting A_0^2 and S from Eqs. (15) and (16) into Eq. (14a), then equating the coefficients of η^2 on both sides of the resulting equation, obtains

$$\varepsilon_0 f \frac{d^2 f}{d\xi^2} = \frac{3 - 2cothn}{f^2} - \Omega^2 \rho_0 \varepsilon_2 - \frac{1}{2} f \frac{df}{d\xi}\frac{d\varepsilon_0}{d\xi} \tag{17}$$

where $\xi = (c/r_0^2\omega)z$ is the dimensionless distance of propagation and $\rho_0 = (r_0\omega/c)$ is the normalized parameter for beam radius.

3. Numerical results and discussion

In the present study, the propagation characteristics of higher-order HshG beams in plasma characterized by ponderomotive nonlinearity have been investigated. These are determined by the modified dielectric function around the maximum of the irradiance on the wavefront of the HshG beams. Evolution Eq. (17) represents a nonlinear differential equation governing the beam-width parameter f of HshG beams in collisionless plasma. The first term on the right-hand side of Eq. (17) characterizes the diffraction divergence of the beam, and the remaining two terms originate from the nonlinear response of the plasma medium. Thus, the nonlinear response of the plasma medium has been analyzed by evaluating dielectric functions $\varepsilon_0(z)$ and $\varepsilon_2(z)$ from Eqs.(13a) and (13b). From Eq.(17), it is clear that the beam-width parameter f will be such that the self-focusing occurs when $d^2f/d\xi^2 < 0$ and the defocusing when $d^2f/d\xi^2 > 0$. A self-trapped mode is thus obvious when the nonlinear response of the plasma exactly balances the diffraction divergence. This is obtained by equating the right-hand side of Eq.(17) to zero by using appropriate initial conditions. We used the fourth-order Runge-Kutta method to solve Eq. (17) with initial conditions $f = 1$ and $df/d\xi = 0$ at $\xi = 0$. To gain deeper insights into the evaluation and propagation behavior of HshG beams in plasma, we have performed a numerical investigation for typical values of parameters of laser produced plasma characterized by Murbat and Hamza [23]. In all analyzed cases, we have supposed Nd:YAG laser system with frequency $\omega = 1.778 \times 10^{15}\, rad/s$ (that corresponds to the laser center wavelength $\lambda = 1.06\, \mu m$) and initial beam radius $r_0 = 20\, \mu m$. We have considered higher-order HshG beams with $n = 2, 4, 6, 8$, initial intensity parameter $p = 0.2 - 0.8$ and normalized plasma frequency $\Omega = 0.6 - 0.9$.
Here, to intuitively understand the initial intensity profile of the laser considered herein, some higher orders of HshG beams are selected to inspect. Correspondingly, the transverse density distributions of intensity configurations of HshG beams with different orders $n = 2, 4, 6, 8$ are shown in Figure 1. The sinh-Gaussian beam exhibits a hollow intensity distribution because a central singularity exists. With the increase in the order n, the hollow region of the HshG laser increases in the transverse plane.

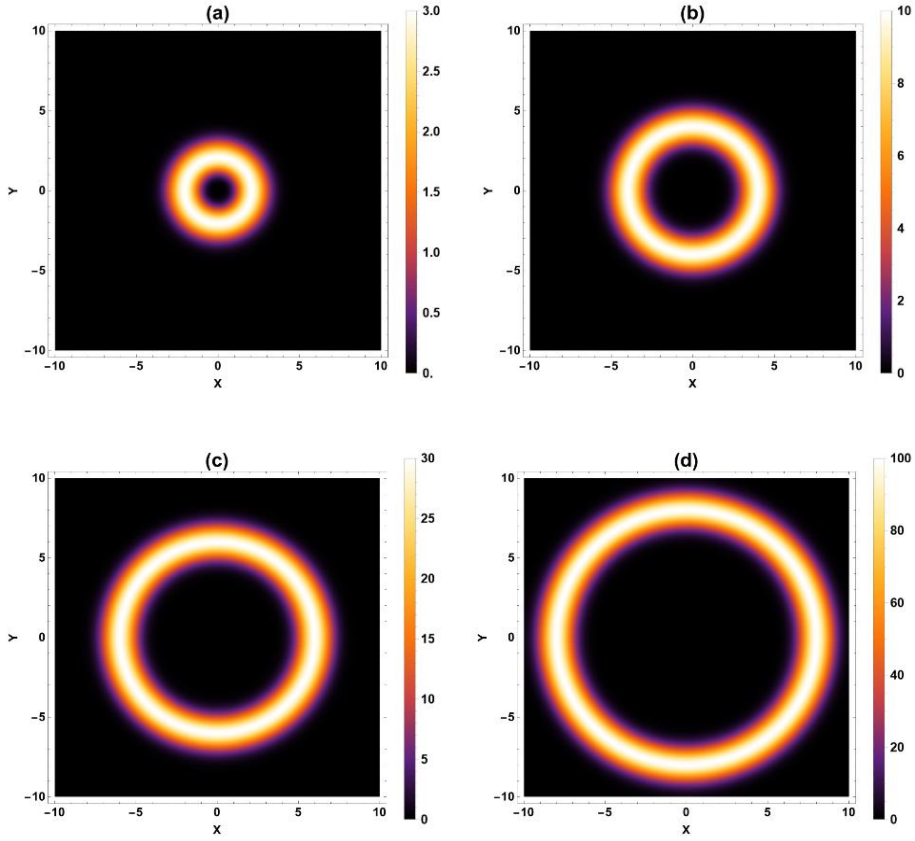

Figure 1. The transverse initial intensity profiles of the HshG beams for different values of order n; (a) $n = 2$, (b) $n = 4$, (c) $n = 6$ and (d) $n = 8$

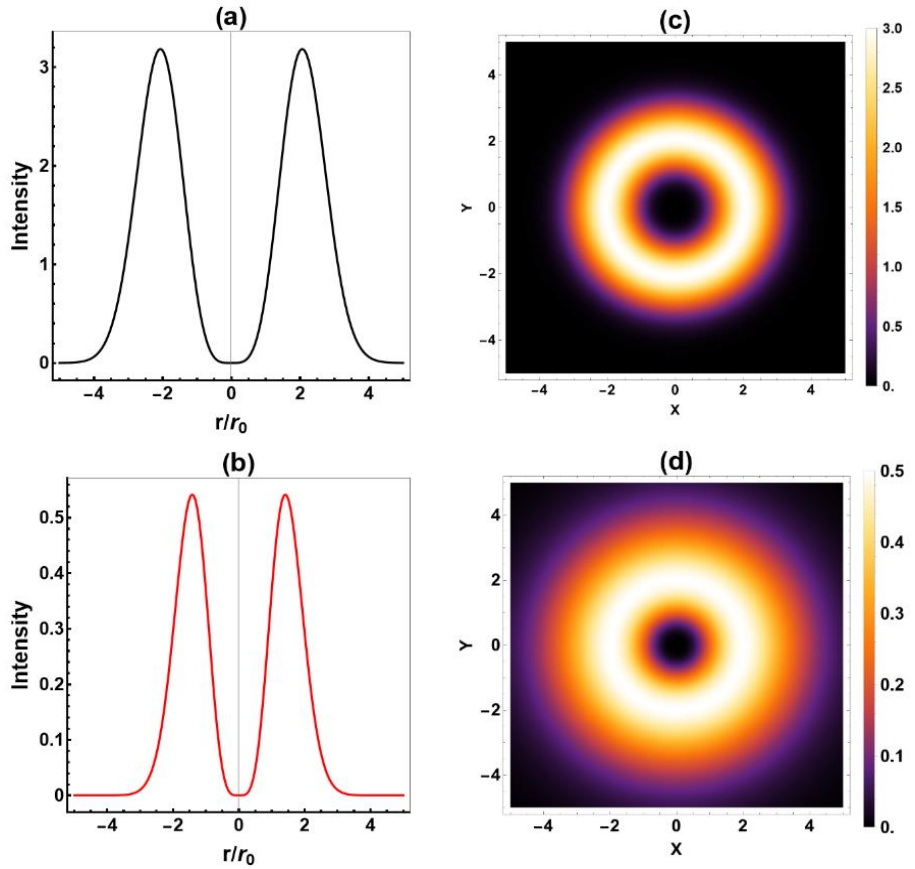

Figure 2. Comparative variation of the normalized intensity profiles of HshG and DHG beams at $n = 2$. Figure (a, c) corresponds to the HshG beam, and Figure (b, d) corresponds to the DHG beam. The first column represents radial intensity distribution, while the second column is for the density dispersal of intensity

10.57647/jtap.2026.2002.17

Such a ring-type structure makes HshG laser beams particularly suitable for studying self-focusing phenomena beyond the conventional near-axis paraxial theory in plasma. Figure 2 illustrates a comparative study of HshG and DHG beams for beam order $n = 2$. The HshG beam Figures 2(a,c) is characterized by a deeper central void and steeper annular walls. This feature originates from the sinh radial dependence, which increases with radial distance and strongly suppresses on-axis intensity. The annular ring becomes more sharply confined, leading to steeper radial intensity and enhanced peak intensity. In contrast, the DHG beam Figures 2(b,d) a broader but relatively shallow hollow core, characteristic of hollow Gaussian profiles. The smoother radial redistribution of energy in the DHG case results in weaker confinement within the ring and substantially lower peak intensity compared to the HshG beam.

Based on the above analysis, it is evident that the propagation characteristics of HshG beams are strongly influenced by the beam order n.

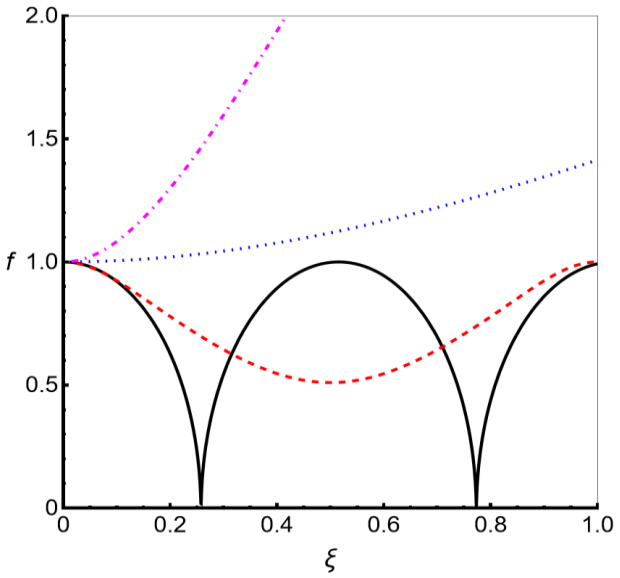

Figure 3. Variation of beam-width parameter f with dimensionless propagation distance ξ for different orders of HshG beams, $n = 2$ (solid curve), $n = 4$ (dashed curve), $n = 6$ (dotted curve) and $n = 8$ (dotted-dash curve). Other numerical parameters are: $r_0 = 20\mu m$, $\omega = 1.77 \times 10^{15}$rad/s, $n_o = 10^{21} cm^{-1}$, Ω =0.8 and $p = 0.5$

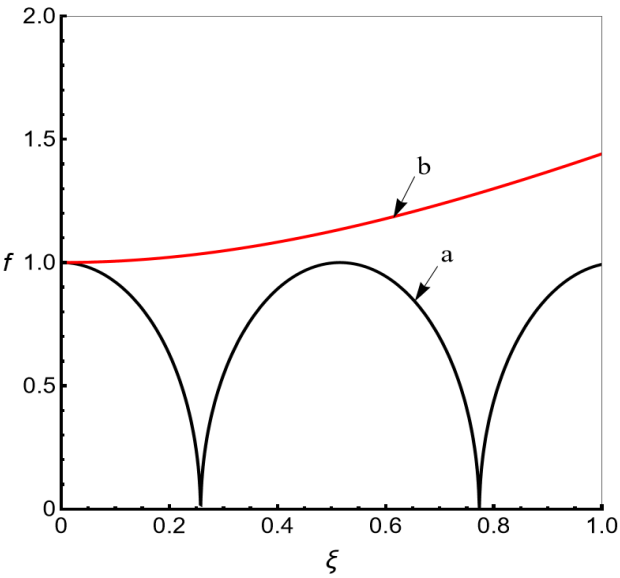

Figure 4. Comparative variation of the beam-width parameter f with the dimensionless propagation distance ξ for HshG and DHG beams at $n = 2$. HshG beam (curve a), DHG beam (curve b). Other numerical parameters are the same as Figure 3

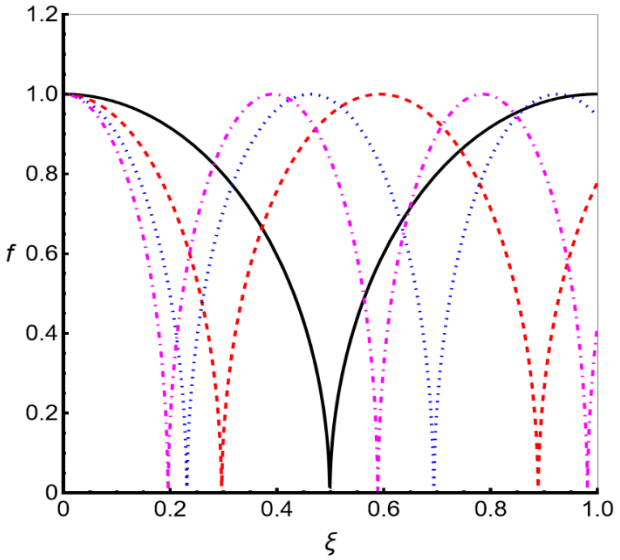

Figure 5. Variation of beam-width parameter f with dimensionless propagation distance ξ for HshG beams with $n = 2$ for different initial intensity parameter values, $p = 0.2$ (solid curve), $p = 0.4$ (dashed curve), $p = 0.6$ (dotted curve) and $p = 0.8$ (dotted-dash curve). Other values of laser-plasma parameters are same as given in Figure 3

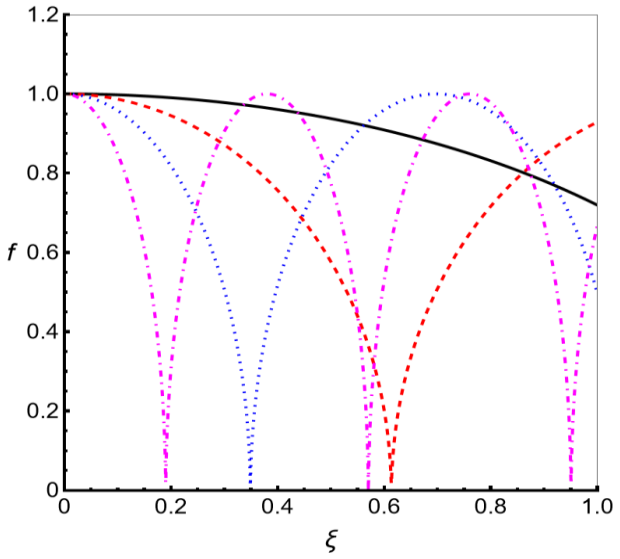

Figure 6. Variation of beam-width parameter f with dimensionless propagation ξ for HshG beams with $n = 2$ for different values of normalized plasma frequency parameter, Ω =0.6 (solid curve), Ω =0.7 (dashed curve), Ω =0.8 (dotted curve) and Ω =0.9 (dotted-dash curve). Other values of laser-plasma parameters are the same as given in Figure 3

10.57647/jtap.2026.2002.17

Figure 3 shows the effect of order n of HshG beams on variation of the beam-width parameter f with dimensionless propagation distance ξ through plasma. It is seen that the self-focusing character is stronger for lower-order HshG beams, while it shows the steady divergence as the order n increases. The dependence of self-focusing on n can be quantified through the nonlinear focal length ξ_f, defined as the propagation distance at which f attains its minimum, serving as an effective measure of the nonlinear response. For $n = 2$, strong self-focusing is observed, with f attaining a deep minimum at $\xi_f \approx 0.25$. For $n = 4$ beam exhibits a minimum at $\xi_f \approx 0.45$ with $f_{min} \approx 0.55$ indicating a longer self-focusing length and reduced nonlinear compression. For $n \geq 6$, the beam-width parameter does not exhibit any well-defined minimum within $0 \leq \xi \leq 1$, remaining $f \geq 1$ throughout propagation, which indicates a strong inhibition of self-focusing. This behavior reflects an increase in the effective critical power P_{cr} with beam order, arising from radial redistribution of intensity and the consequent reduction of the transverse ponderomotive force gradient. The comparative variation of the beam-width parameter f with the dimensionless propagation distance ξ for HshG and DHG beams at $n = 2$ is shown in Figure 4. Due to strong nonlinear self-focusing, the HshG beam (curve a) exhibits pronounced oscillations in f, whereas the DHG beam (curve b) maintains its beam width nearly constant, indicating a smaller plasma perturbation. This indicates that, for the same beam order, the HshG beam experiences significantly stronger nonlinear self-focusing compared to the DHG beam.

The variation of the dimensionless beam-width parameter f on the propagation distance ξ for $n = 2$ of HshG beams for different values of the initial intensity parameter $p = 0.2, 0.4, 0.6, 0.8$ for a fixed value of the normalized plasma frequency parameter $\Omega = 0.8$ has been displayed in Figure 5. The plot indicates that HshG beams undergo stronger focusing, accompanied by a decrease in self-focusing length with increasing intensity parameter. The reason behind this is that the nonlinear nature of the plasma medium is directly dependent on the intensity of the laser. Thus, further increasing the self-focusing of HshG beams is observed.

Figure 6 indicates the variation of beam-width parameter f on the propagation distance ξ for $n = 2$ of HshG beams for different values of normalized plasma frequency $\Omega = 0.6, 0.7, 0.8, 0.9$ and keeping the initial intensity parameter $p = 0.5$ constant. It has been observed that HshG beams get more focused with an increase in plasma frequency. This is due to the fact that with an increase in the value of plasma frequency, the density of plasma electrons increases.

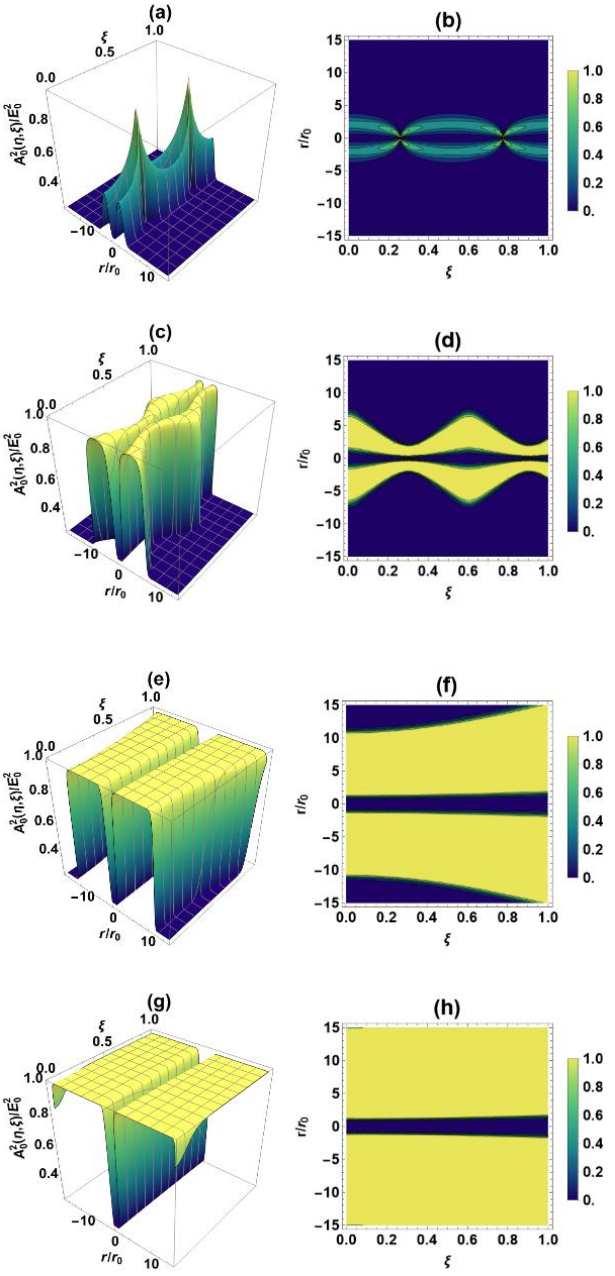

Figure 7. Dependence of normalized intensity of HshG beams with radial distance r/r_0 and the distance of propagation ξ for different values of order n, (a) $n = 2$, (c) $n = 4$, (e) $n = 6$, and (g) $n = 8$. Corresponding contour plots are (b) $n = 2$, (d) $n = 4$, (f) $n = 6$, and (h) $n = 8$

Consequently, more plasma electrons are available for participation in the nonlinear behavior of the plasma medium, and thus, significantly increased self-focusing behavior of HshG beams with further reduction in self-focusing length is observed.

To further elucidate the results for delineating the underlying physics for the propagation characteristics of HshG beams in collisionless plasma, we numerically analyze the dependence of normalized intensity distributions of HshG beams for different n-values. Figure 7 shows the variation of normalized intensity of HshG beams with normalized radial distance r/r_0 and the

distance of propagation ξ for different orders $n = 2, 4, 6, 8$. Intensity profiles in Figure 7 are of reasonably high relevance to explore self-focusing and defocusing characteristics of HshG beams in plasma. We see clearly that low-order HshG beams present strongly localized oscillatory behavior of intensity distribution around the propagation axis. Such an oscillatory configuration broadens in the transverse plane, giving rise to a maintained hollow-core structure with propagation distance as order n of HshG beams increases. These results are in conformance with the self-focusing and defocusing behavior of HshG beams shown in Figure 3. Figure 8 illustrates the evolution of the normalized intensity with radial distance r/r_0 and propagation distance ξ for beam order $n = 2$.

The HshG beam Figures (a, b) show that the HshG beam exhibits pronounced radial oscillations and compression due to its steep transverse intensity, enhancing the ponderomotive nonlinearity. In contrast, the DHG beam Figures (c, d) exhibits a nearly invariant hollow structure during propagation and shows a minor dependence on ξ. Due to its lower plasma density perturbation and finer radial profile, the DHG beam exhibits less intensity modulation. Therefore, the HshG beam experiences far more nonlinear self-focusing than the DHG beam for the same beam order n.

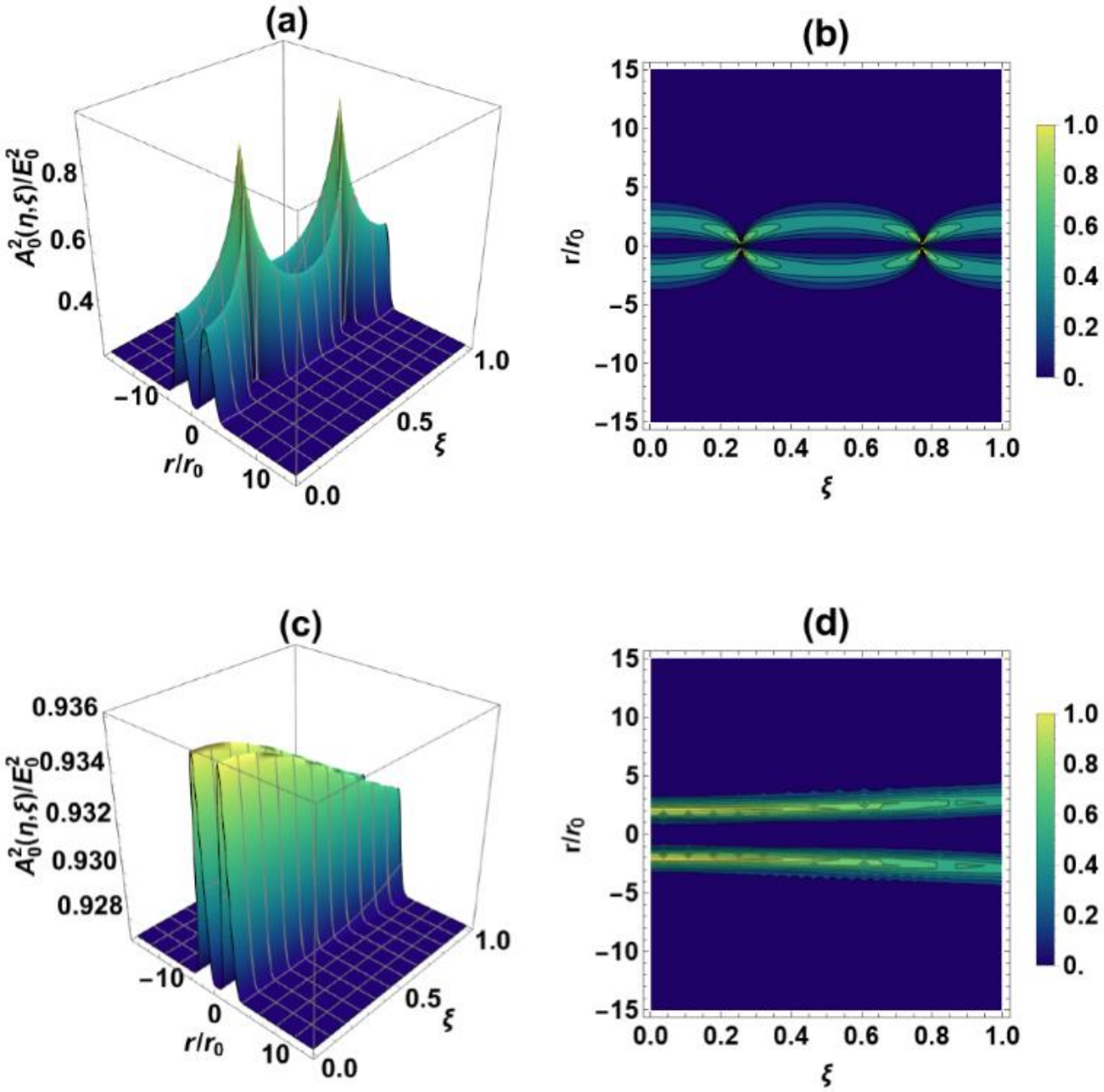

Figure 8. Comparative plots showing the dependence of the normalized intensity of HshG and DHG beams on the radial distance r/r_0 and the propagation distance ξ for order $n = 2$. Figure (a, b) corresponds to the HshG beams, while Figure (c, d) represents the DHG beams

10.57647/jtap.2026.2002.17

4. Conclusion

In this study, we have investigated the propagation characteristics of higher-order sinh-Gaussian (HshG) laser beams in plasma characterized by ponderomotive nonlinearity. The modified paraxial approach is employed to expand the relevant parameters around the maximum of irradiance. The nonlinear differential equation for the beam-width parameter of HshG beams is obtained by mainly determining the dielectric function of plasma. Finally, the obtained evolution equation is solved numerically by using the fourth-order Runge–Kutta method for typical values of laser-plasma parameters. It is found that the self-focusing ability of HshG beams weakens noticeably as the beam order increases. In addition, HshG beams show improved self-focusing with an increase in the intensity parameter and the normalized parameter of plasma frequency. The outcome of the present investigation is expected to contribute significantly to the recent advancement in the understanding of the interaction of ring-shaped laser beams with plasma under different physical situations of interest.

Declarations

Funding
This research received no external funding.

Authors Contribution
All the authors have participated sufficiently in the intellectual content, conception and design of this work or the analysis and interpretation of the data, as well as the writing of the manuscript.

Availability of data and materials
Data will be made available upon reasonable request to the corresponding author.

Conflict of interests
The authors declare no conflict of interest.

References

[1] T. Baeva, S. Gordienko, A. Pukhov, Theory of high-order harmonic generation in relativistic laser interaction with overdense plasma, *Phys. Rev. E* 74 (2006) 046404.

[2] V.T. Tikhonchuk, Physics of laser plasma interaction and particle transport in the context of inertial confinement fusion, *Nucl. Fusion* 59 (2019) 032001.

[3] M.S. Dorozkina, K.V. Baluev, D.D. Kutergin, I.K. Lotov, V.A. Minakov, R.I. Spitsyn, P.V. Tuev, K.V. Lotov, Laser wakefield acceleration in a plasma channel, *Bull. Labedev Phys. Inst.* 50 (2023) S715-S723.

[4] A. Kumar, K. Gopal, Terahertz Radiation Generation from Beat Laser Interaction with Step Density Rippled Plasma, *IEEE Trans. Plasma Sci.* 52 (2024) 3029-3036.

[5] P.J. Delfyett, D. Mandridis, M. Piracha, D. Nguyen, K. Kim, S. Lee, Chirped pulse laser sources and applications, *Prog Quant. Electron.* 36 (2012) 475-540 .

[6] S.A. Akhmanov, A.P. Sukhorukov, R.V. Khokhlov, Self-focusing and diffraction of light in a nonlinear medium, *Sov. Phys. Usp.* 10 (1968) 609-636.

[7] M.S. Sodha, A.K. Ghatak, V.K. Tripathi, Self-focusing of laser beams in plasmas and semiconductors, *Prog. Opt.* 13 (1976) 169-265.

[8] S.D. Patil, M.V. Takale, S.T. Navare, V.J. Fulari, M.B. Dongare, Analytical study of HChG-laser beam propagation in collisional and collisionless plasmas, *J. Opt.* 36 (2007) 136-144.

[9] Y. Cai, C. Chain, F. Wang, Hollow Gaussian beams and their propagation properties, *Opt. Lett.* 28 (2003) 1084-1086.

[10] Y. Cai, C. Chain, F. Wang, Modified hollow Gaussian beam and its paraxial propagation, *Opt. Commun.* 278 (2007) 34-41.

[11] M.S. Sodha, S.K. Misra, S. Mishra, Focusing of dark hollow Gaussian Electromagnetic beams in plasma, *Laser Part. Beams* 27 (2009) 57-58.

[12] C. Tan, X. Fu, Y. Deng, Generation of ring-shaped beams by a graded-index plasma lens, *J. Opt.* 15 (2013) 125202.

[13] A. Sharma, M. S. Sodha, S. Misra, S.K. Mishra, Thermal defocusing of intense hollow Gaussian laser beams in atmosphere, *Laser Part. Beams* 31 (2013) 403-410.

[14] X.-R. Hong, Y.-L. Zheng, R.-A. Tang, T.-F. Liu, X.-P. Liu, Propagation characteristics of a hollow Gaussian laser beam in a tapered plasma channel, *Phys. Plasmas* 27 (2020) 043109 .

[15] M. Hashemzadeh, M. Abbasi-Firouzjah, Second-harmonic generation of hollow Gaussian laser beams in inhomogeneous plasmas in the presence of wiggler magnetic field, *Waves Random Complex Media* 34 (2021) 2567-2581.

[16] G. Purohit, Upper hybrid wave excitation and particle acceleration by resonant beating of two hollow Gaussian laser beams in magnetized plasma, *J. Opt. Soc. Am. B* 39 (2022) 2066-2073.

[17] C. Brabetz, S. Busold, T. Cowan, O. Deppert, D. Jahn, O. Kester, M. Roth, D. Schumacher, V. Bagnoud, Laser-driven ion acceleration with hollow laser beams. *Phys. Plasmas* 22 (2015) 013105.

[18] H. K. Malik, S. Punia, Dark hollow beams originating terahertz radiation in corrugated plasma under magnetic field, *Phys. Plasmas* 26 (2019) 063102.

[19] Q. Sun, K. Zhou, G. Fang, G. Zhang, Z. Liu, S. Liu, Hollow sinh-Gaussian beams and their paraxial properties, *Opt Exp.* 20 (2012) 9682-9691.

[20] B. Tang, S. Jiang, C. Jiang, H. Zhu, Propagation properties of hollow sinh-Gaussian beams through Fractional Fourier Transform optical systems, *Opt. Laser Technol.* 59 (2014) 116-122.

[21] D. Zou, X. Li, X. Pang, H. Zheng, Y. Ge, Propagation properties of hollow sinh-Gaussian beams in quadratic-index medium, *Opt. Commun.* 401(2017) 54-58.

[22] K. Zhu, R. Liang, Y. Yi, J. Zhu, H. Tang, Propagation invariance and dark hollow structures of sinh-Gaussian beams with small complex parameters, *J. Phys. Conf. Ser.* 1732 (2021) 012163.

[23] H.H. Murbat, H.A. Hamza, The influence of Nd: YAG laser energy on plasma characteristics produced on Si:Al alloy target in atmospheric pressure, *J. Mater. Sci. Appl.* 3(20147) 1-7.

10.57647/jtap.2026.2002.17